



Atf için / For Citation: N. Sedefoğlu, H. Kavak, "Electrochemical and structural behavior of Bi doped ZnO materials obtained with solvothermal synthesis method", *Süleyman Demirel Üniversitesi Fen Edebiyat Fakültesi Fen Dergisi*, 16(1), 147-156, 2021.

## Electrochemical and Structural Behavior of Bi Doped ZnO Materials Obtained with Solvothermal Synthesis Method

Nazmi SEDEFOĞLU<sup>\*1</sup>, Hamide KAVAK<sup>2</sup>

<sup>1</sup>*Osmaniye Korkut Ata University, Arts and Science Faculty, Department of Physics, 80000, Osmaniye, Turkey*

<sup>2</sup>*Çukurova University, Arts and Science Faculty, Department of Physics, 01330, Adana, Turkey*

*\*corresponding author e-mail: nazmisedefoglu@osmaniye.edu.tr*

*(Alınış / Received: 24.02.2021, Kabul / Accepted: 13.04.2021, Yayınlanma / Published: 27.05.2021)*

**Abstract:** In this study, Bi-doped ZnO and undoped ZnO nanomaterials have been synthesized by the solvothermal reaction method. The effect of Bi doping on the structural and electrochemical properties has been investigated by X-ray diffractions (XRD), X-ray photoelectron spectroscopy (XPS) and, scanning electron microscopy (SEM). As seen from X-ray diffraction spectra performed on the bulk material, it has been clearly observed that both Bi doping changed the preferred orientation of the nanopowder as (101) and Bi<sup>+3</sup> ions were expectedly entered the lattice. Furthermore, this result has been supported by photoelectron spectra. Scanning electron microscopy images have shown the shapes and distributions of nanostructures of the samples. As a result, it is thought that Bi doping is suitable for obtaining p-type conductivity in ZnO materials for the experimental processes we applied to samples in the study.

**Key words:** ZnO: Bi, Bi doping, Solvothermal synthesis

### Solvotermal Sentezleme Yöntemi ile Elde Edilen Bi Katkılı ZnO Malzemelerinin Elektrokimyasal ve Yapısal Davranışı

**Özet:** Bu çalışmada, Bi katkılı ZnO ve katkisiz ZnO nanomateryaller solvotermal reaksiyon yöntemi ile sentezlenmiştir. Bi katkısının yapısal ve elektrokimyasal özellikler üzerindeki etkisi X-ışını kırınımları (XRD), X-ışını fotoelektron spektroskopisi (XPS) ve taramalı elektron mikroskobu (SEM) ile araştırılmıştır. Katı malzeme üzerinde gerçekleştirilen X-ışını kırınım spektrumlarından görüldüğü üzere, hem Bi katkılama nanotozun tercih edilen yöneliminin (101) olarak değiştirdiğini hem de Bi<sup>+3</sup> iyonlarının beklenen şekilde kristal kafese girdiği açıkça gözlemlenmiştir. Ayrıca, bu sonuç fotoelektron spektrumları ile desteklenmiştir. Taramalı elektron mikroskobu görüntüleri, numunelerin nanoyapılarının şekillerini ve dağılımlarını göstermiştir. Sonuç olarak, çalışmada numunelere uyguladığımız deneysel işlemler için Bi katkılamanın ZnO malzemelerde p tipi iletkenliğin elde edilmesi bakımından uygun olduğu düşünülmektedir.

**Anahtar kelimeler:** ZnO:Bi, Bi katkılama, Solvotermal sentezleme

## 1.Introduction

ZnO is an important II-VI compound semiconductor with a wide direct bandgap, because of these properties it is considered a very important candidate for some application in optoelectronic devices like light-emitting diodes, laser diodes, flat panel, and photo-detectors [1-7]. It is important such application that to fabricate n-type and p-type stable ZnO however, intrinsic ZnO is n-type conductive due to native defect in the structure like oxygen vacancy, interstitial zinc, and hydrogen impurities [8]. To overcome the effect of the native defect on p-type conductivity, doping is the most convenient option. In recent years there are many groups works on p-type doping and many reports have been published on doping with group V element. Limpijumnong et al. [9] proposed  $X_{Zn}-2V_{Zn}$  acceptor model about the large-size-mismatched impurities in ZnO. This mechanism stems from the low formation enthalpy of  $X_{Zn}-2V_{Zn}$  complexes and X atoms occupy Zn antisite rather than O site.

In recent years, many experiments are conducted on group V element doping in ZnO like N [10, 11], P [12], As [13], and Sb [14] but there is very little paper are reported on bismuth doping in ZnO.  $Bi_{Zn}-2V_{Zn}$  mechanism is not deeply discussed and not enough evidence on the type of conductivity of Bi:ZnO. Moreover, their structural and electrochemical characteristics are not fully understood.

Hydrothermal synthesis refers to the use of water in the reaction as a solvent. solvothermal synthesis which typically uses other solvents including ethylene glycol, ethanol, acetone, and oleic acid is a broader terminology.

In this work, Bi-doped ZnO with solvothermal synthesis. There are many ways to produce that this nanostructure but solvothermal synthesis is mostly the preferred method because of its simplicity, the capability of large-scale production, and low-temperature production [15-18]. And, doping mechanism of Bi into ZnO will be investigated by various methods. Moreover, in this work, samples are produced at 150 °C which is the optimum growth temperature for this synthesis.

## 2.Material and Method

Bismuth doped zinc oxide samples were prepared by the solvothermal solution synthesis method. All chemicals in the synthesis were analytic-grade reagents. In this experiment zinc nitrate hexahydrate  $Zn(NO_3)_2 \cdot 6H_2O$  was used as a starting material. DI (distilled) water and acetone were used as a solvent. Hexamethylenetetramine ( $C_6H_{12}N_4$ ) and bismuth chloride ( $BiCl_3$ ) were used as stabilizers and dopant sources respectively. The concentration which is  $Bi^{+3}$  molar percentage in the solution was changed from 0 to 10 at % in the solution. The mixture was magnetically stirred for 1 h to get a homogeneous solution. Then the solution was put into the Teflon liners, and heated to 150 °C for 24 h, and cooled down to room temperature  $0.1\text{ }^\circ\text{C}/\text{min}$ .

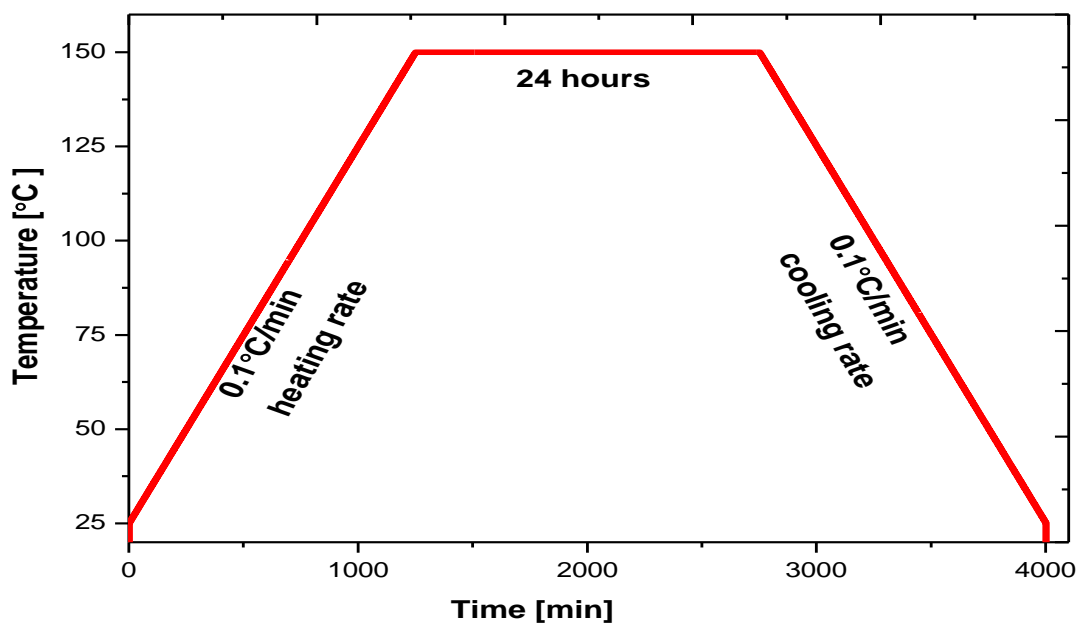


**Figure 1.** Synthesis graph for reactions time (min) vs temperature (°C)

The residual solution was filtered and rinsed with DI water and dried at 90 °C in the air for an hour, after then dried powder calcinated at 800 °C for 12 h as shown in Figure 1 schematically. X-ray powder diffraction analysis of Bi-doped ZnO was performed at room temperature in the angular range of  $2\theta = 20^\circ\text{--}70^\circ$  with a scan step width of  $0.02^\circ$  and a fixed counting time of 1 s/step using an automated Rigaku Ultima IV X-ray diffractometer equipped with Cu  $K\alpha$  radiation of wavelength  $\lambda = 1.5418 \text{ \AA}$ . Crystallite sizes are calculated with Scherrer's method using the (101) orientation of ZnO. X-ray photoelectron spectroscopy was used to analyze the compositional properties of the sample with Thermo Scientific ESCALAB 250Xi. Pass energy and step within XPS measurements are 50 eV and 0.1 eV respectively. SEM image has been taken from Hitachi SU8030.

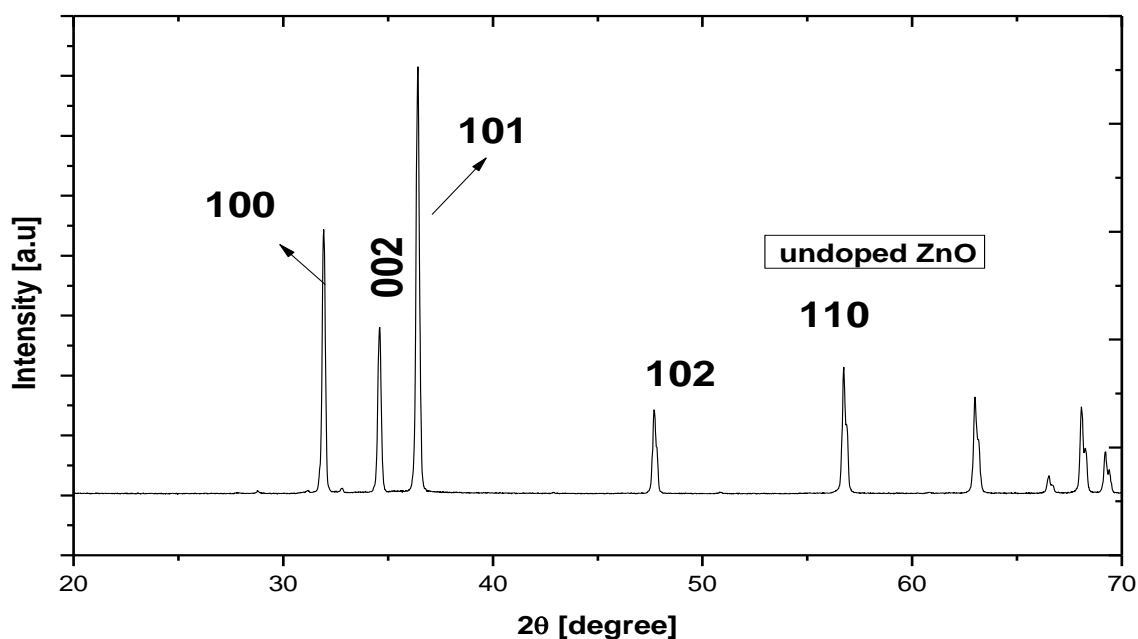


**Figure 2.** X-ray diffraction pattern of undoped ZnO sample

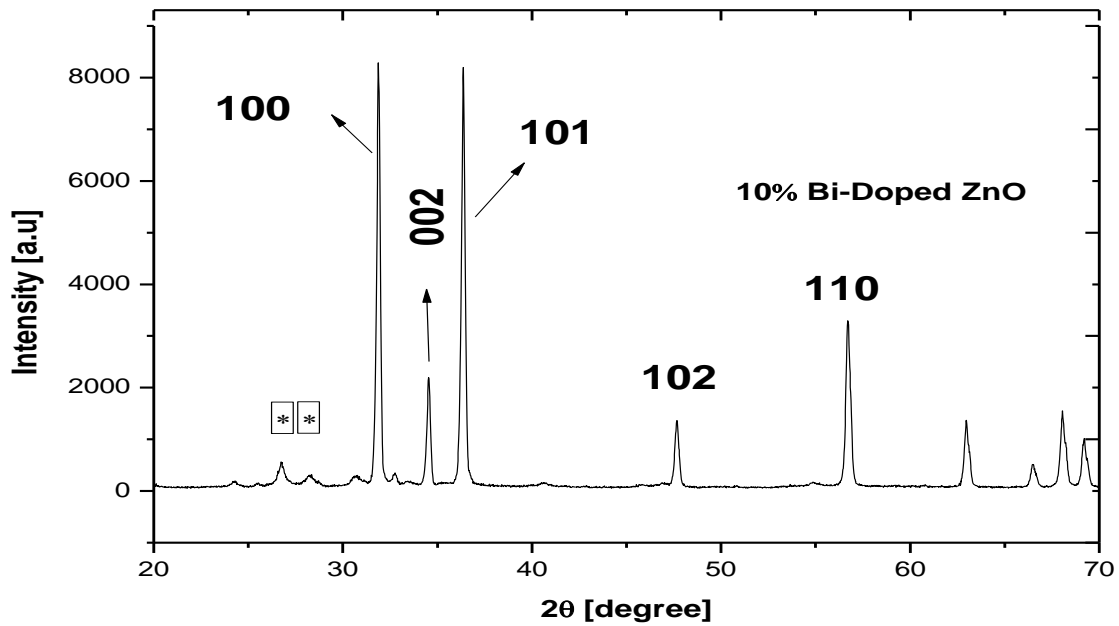
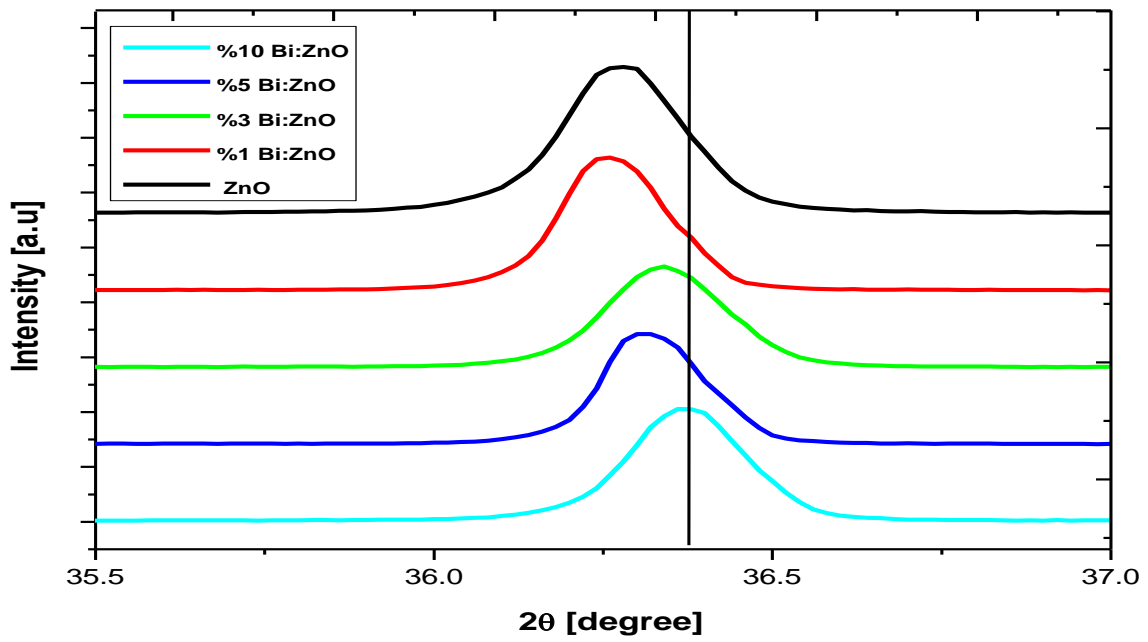


Figure 3. X-ray diffraction pattern of 10% Bi-doped ZnO sample \* shows secondary phases

### 3.Result and Discussion

XRD patterns of the undoped and Bi-doped samples are shown in Figures 2-5. Figure 2 shows the undoped XRD pattern of ZnO which crystallized in hexagonal wurtzite structure in mixed-orientation and all diffraction peaks can be indexed as standard wurtzite ZnO [19]. Undoped, 1% and 3% Bi-doped ZnO samples show only standard wurtzite ZnO peaks, there is not any secondary diffraction peak however 5 % and 10 % Bi-doped ZnO shows some secondary peaks as in Figure 5 and Figure 3. Moreover, Figure 5 shows that increasing the doping concentration causes a slight decrease in the (002) diffraction peak as reported by Kumar et al. [20] and increased the (101) diffraction peaks. This increment on (101) shows that increasing the doping concentration changes the preferred orientation of ZnO [21]. The shift is shown in Figure 4 also indicates that  $\text{Bi}^{+3}$  ions are substituted into the  $\text{Zn}^{+2}$  ions site and [22]. Additionally, doping the materials with a bigger ionic radius causes a shift to higher angles in XRD diffraction peaks. This estimation is also supported by a previous study that mentions the huge differences between the atomic radius of  $\text{Bi}^{+3}$  (1.20 Å) and  $\text{Zn}^{+2}$  (0.74 Å) [23].



**Figure 4.** XRD diffraction pattern of (101) diffraction peaks of undoped and Bi-doped ZnO sample

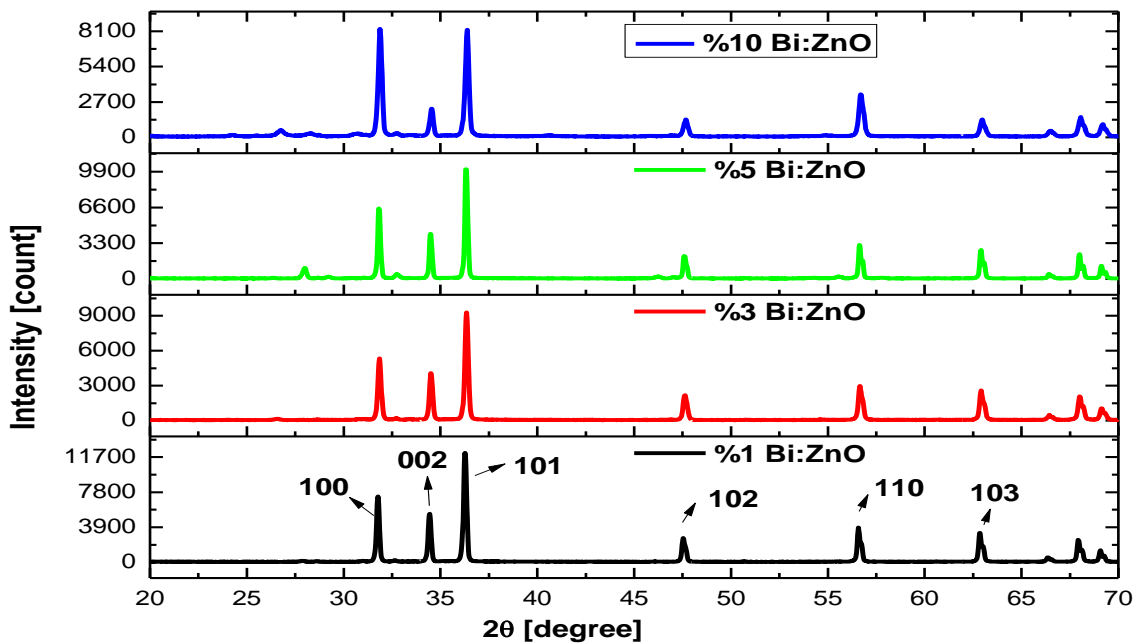


**Figure 5.** XRD diffraction pattern of Bi-doped ZnO samples

FWHM of the samples given in Figure 6, shifts to the higher angles with an increment of Bi doping. The measured FWHM value for (101) diffraction peaks was measured as 0.140 for pure ZnO and 0.182 for the % 10 Bi-doped ZnO. Similarly, it was observed that the FWHM values of the (100) and (002) diffraction peaks increased with the increase in the doping ratio. These results also verify that Bi atoms are successfully doped into the ZnO lattice and cause lattice expansions in the ZnO crystals [19, 24]. The crystallite size of the samples was determined by the Debye-Scherer formula given in Eq. 1 [25]:

$$d = \frac{K \cdot \lambda}{\beta \cos \theta_{hkl}} \quad (1)$$

where  $\lambda$  is the wavelength of XRD,  $\beta$  is the FWHM of the selected peak K is a constant which is taken as 0.9 and  $\theta$  is the Bragg angle of a selected peak. For (101), the crystallite size of ZnO samples slightly alters from 7.84 nm for %10 Bi: ZnO to 9.95 nm for pure ZnO.

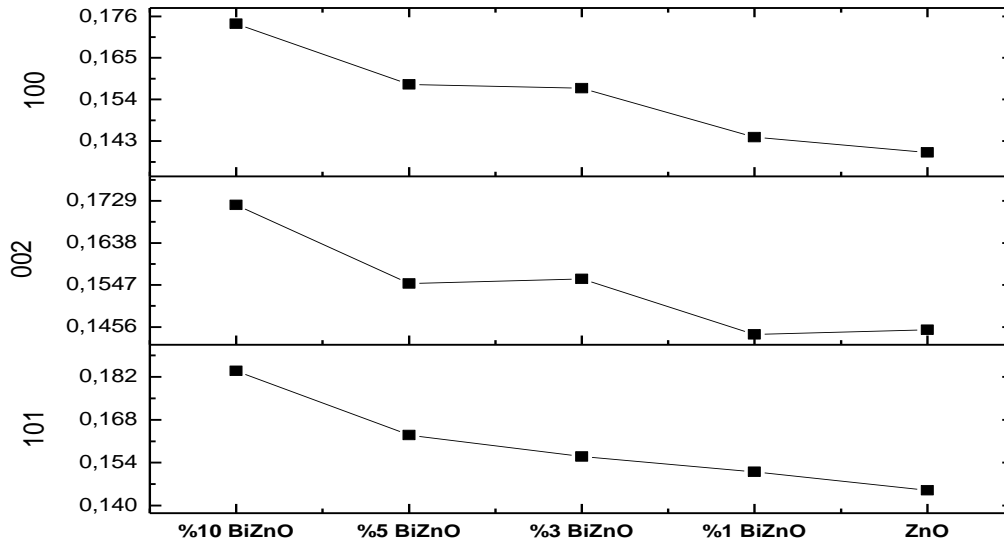


**Figure 6.** FWHM values of Bi<sup>+3</sup> doped and undoped ZnO samples for [101, 002, 100] orientation

XPS was used to characterize the electrochemical composition of the ZnO: Bi samples. XPS spectra of Bi-doped ZnO are placed in Figure 7. In Figures 7 a, b, c, and d, it can be seen that 4f core-level spectra of 1, 3, 5, and 10% doped ZnO respectively. And Figure 7 e and f show us Carbon 1s core-level spectra and survey compositional analysis of 10% doped ZnO respectively. C 1s peaks are used to calibrate the spectra. C 1s peaks are settled to 284.6 eV for each sample [26]. According to Figure 7, there is an inversely proportional ratio between the doping concentration and Bi 4f core-level spectra peaks. As can be seen, while doping concentration increased, the location of Bi 4f<sub>5/2</sub> decreased from 159.4 to 158.4. Also, Bi 4f<sub>7/2</sub> peaks locations in the spectra are decreased. There are no Bi 4f<sub>7/2</sub> peaks on the XPS spectra located below the 157 eV. This shows us Bi-O bonding was established rather than Zn-Bi bonding in the lattice accordingly Xu et al. [27]. Bi 4f<sub>7/2</sub> peaks located about 163.7 eV showed that Bi<sup>+3</sup> is the major charge state and BiO is produced in the Bi-doped ZnO by substituting for Zn as Bi<sub>Zn</sub> [27, 28]. The shift of the peaks may be caused by changing electromagnetic field inside the sample [29]. XPS and XRD measurements are in compliance with each other.

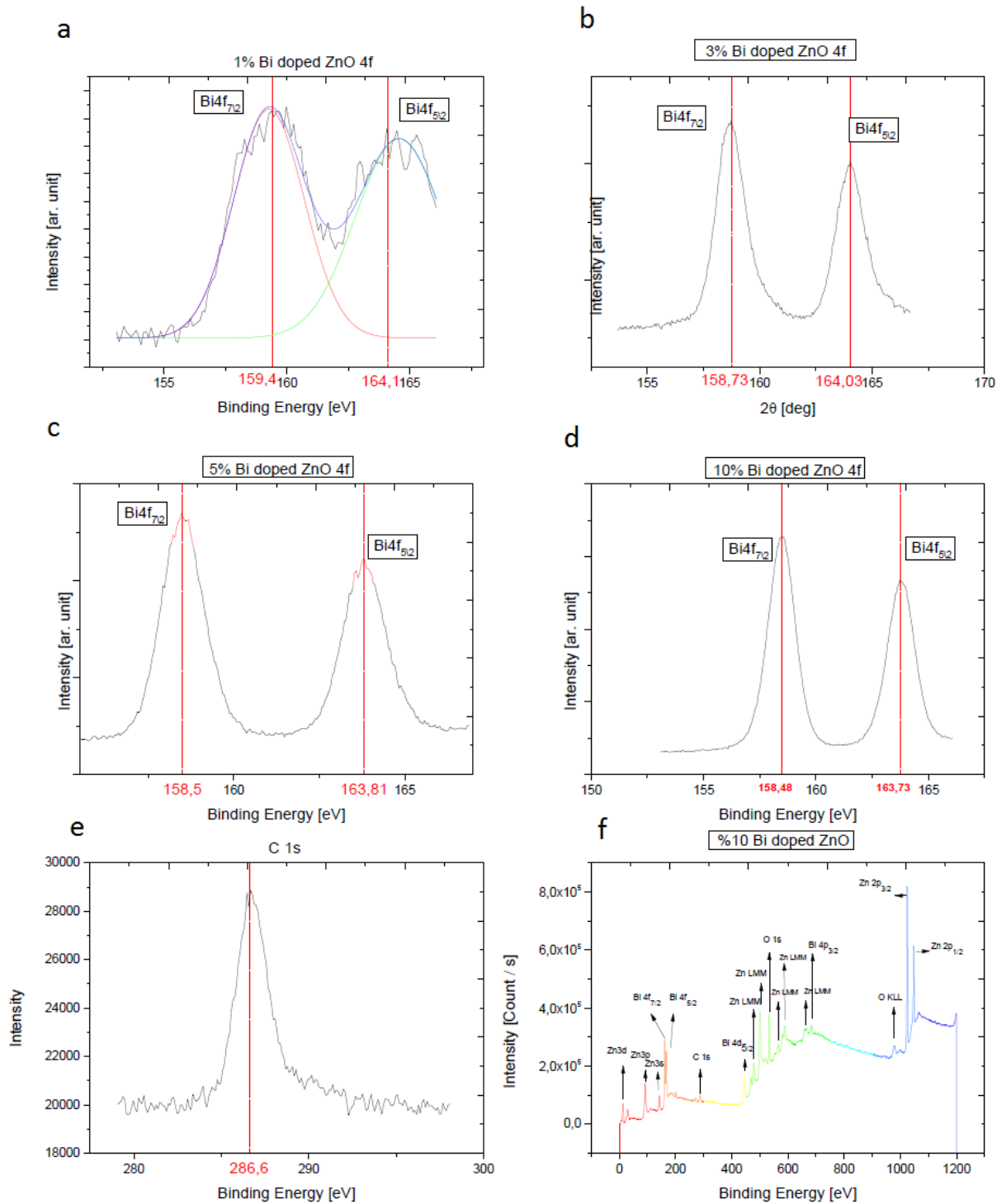


**Figure 7.** XPS core-level spectra of Bi-doped ZnO a) b) c) d) is the 4f core-level spectra of Bi for 1, 3, 5, and 10 % doped ZnO respectively e) f) is the C 1s core-level spectra and survey spectra of 10 % doped ZnO

As seen in the SEM images (Figures 8, 9), particles with a size of 1-2  $\mu\text{m}$  and less than 1  $\mu\text{m}$  appear to have formed nonhomogeneous. The planes on the surfaces of the particles are noticed and it can be said that they have a hexagonal structure. It is seen that the particles have different orientations, angle differences, and large thick bars on their surfaces. When examined in Figure. 8, it is thought that small particles come together to form these large heaps.

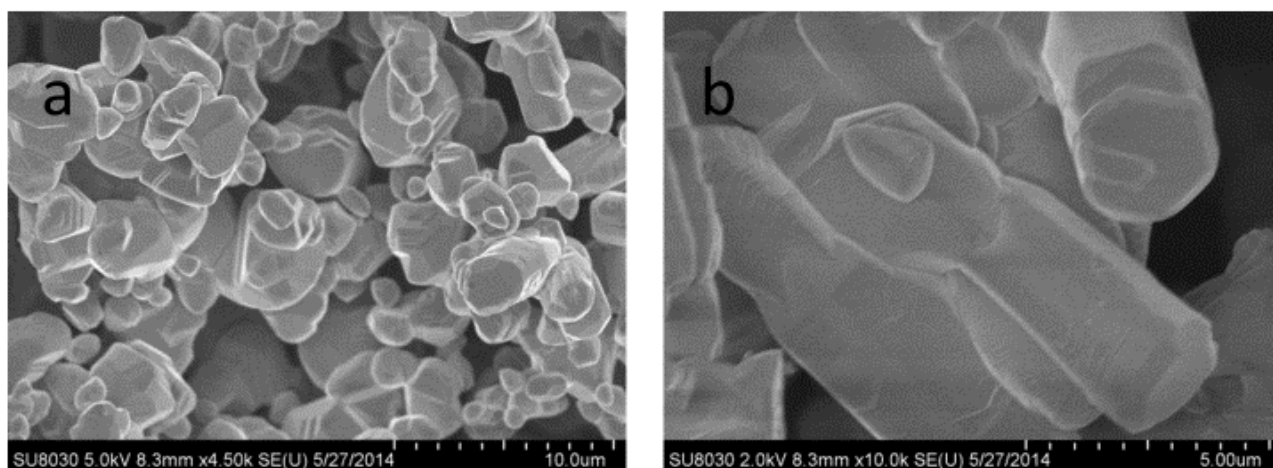


**Figure 8.** SEM image of 3% Bi:ZnO sample a) with 4500X b) 10000X magnification



**Figure 9.** SEM image of pure ZnO sample with 35000X magnification

#### 4. Conclusion and Comment

The ZnO: Bi samples were synthesized by the solvothermal synthesis method and calcinated 800 °C for 12 hours in the air atmosphere. The XRD patterns showed that Bi doping was successful and the change in doping concentration has improved the crystal quality up to 5%. After this doping concentration was exceeded, secondary phases were observed. Further, XRD peaks of (101) orientation shifted to higher angles with increasing doping concentration. Additionally, while the concentration of Bi doping in the samples was increased, (101) diffraction peaks intensity was increased but the intensity of (002) peaks was decreased which are interpreted as doping were achieved. The XPS results showed that the dopant atoms replaced the Zn atoms in the lattice, producing the  $\text{Bi}_{\text{Zn}}$  defect. In XPS measurement, there was not any Bi 4f<sub>7/2</sub> peaks lower than 157 eV which means  $\text{Bi}^{+3}$  is the preferred oxidation state. Lastly, from these given

XPS results, it is concluded that the  $\text{Bi}^{+3}$  ion is a suitable candidate to form the  $\text{X}_{\text{Zn}}-2\text{V}_{\text{Zn}}$  complex and successfully produced in this study.

### Author Statement

Nazmi SEDEFOGLU: Methodology, Investigation, Review and Editing, Conceptualization, Investigation, Original Draft Writing

Hamide KAVAK: Methodology, Supervision, Observation, Advice

### Acknowledgment

This study has been financially supported by the Department of Scientific Research Project (BAP) of Çukurova University as project number FEF2013D30.

### Conflict of Interest

As the authors of this study, we declare that I do not have any conflict of interest statement.

### Ethics Committee Approval and Informed Consent

As the authors of this study, we declare that I do not have any ethics committee approval and/or informed consent statement.

### References

- [1] D. C. Look, "Recent advances in ZnO materials and devices," *Mater. Sci. Eng., B*, 80, 383-387, 2001.
- [2] H. Kim, J. S. Horwitz, W. H. Kim, A. J. Makinen, Z. H. Kafafi, and D. B. Chrisey, "Doped ZnO thin films as anode materials for organic light-emitting diodes," *Thin Solid Films*, 420, 539-543, 2002.
- [3] C. Yuen, S. F. Yu, S. P. Lau, and G. C. K. Chen, "Design and fabrication of ZnO light-emitting devices using filtered cathodic vacuum arc technique," *J. Cryst. Growth*, 287, 204-212, 2006.
- [4] F. C. M. Vandepol, "Thin Film ZnO - properties and applications," *Am. Ceram. Soc. Bull.*, 69, 1959-1965, 1990.
- [5] R.-Y. Yang, M.-H. Weng, C.-T. Pan, C.-M. Hsiung, and C.-C. Huang, "Low-temperature deposited ZnO thin films on the flexible substrate by cathodic vacuum arc technology," *Appl. Surf. Sci.*, 257, 7119-7122, 2011.
- [6] K. Chung, C.-H. Lee, and G.-C. Yi, "Transferable GaN layers grown on ZnO-coated graphene layers for optoelectronic devices," *Sci.*, 330, 655-657, 2010.
- [7] M. H. Huang, S. Mao, H. Feick, H. Q. Yan, Y. Y. Wu, H. Kind, *et al.*, "Room-temperature ultraviolet nanowire nanolasers," *Sci.*, 292, 1897-1899, 2001.
- [8] S. B. Zhang, S. H. Wei, and A. Zunger, "Intrinsic n-type versus p-type doping asymmetry and the defect physics of ZnO," *Phys. Rev. B*, 63 (7), 075205, 2001.
- [9] S. Limpijumnong, S. B. Zhang, S. H. Wei, and C. H. Park, "Doping by large-size-mismatched impurities: The microscopic origin of arsenic- or antimony-doped p-type zinc oxide," *Phys. Rev. Lett.*, 92 (15), 155504, 2004.
- [10] P. Sikam, C. Sararat, P. Moontragoon, T. Kaewmaraya, and S. Maensiri, "Enhanced thermoelectric properties of N-doped ZnO and SrTiO<sub>3</sub>: A first-principles study," *Appl. Surf. Sci.*, 446, 47-58, 2018.
- [11] M. Moalem-Banhangi, N. Ghaeni, and S. Ghasemi, "Saffron derived carbon quantum dot/N-doped ZnO/fulvic acid nanocomposite for sonocatalytic degradation of methylene blue," *Synth. Met.*, 271, 116626, 2021.
- [12] S. Swathi, R. Yuvakkumar, G. Ravi, E. S. Babu, D. Velauthapillai, and S. A. Alharbi, "Morphological exploration of chemical vapor-deposited P-doped ZnO nanorods for efficient photoelectrochemical water splitting," *Ceram. Int.*, 47 (5), 6521-6527, 2021.
- [13] S. Y. Wakhare and M. D. Deshpande, "Structural, electronic and optical properties of metalloid element (B, Si, Ge, As, Sb, and Te) doped g-ZnO monolayer: A DFT study," *J. Mol. Graph. Model.*, 101, 107753, 2020.
- [14] C.-Q. Luo, S.-C. Zhu, C. Xu, S. Zhou, C.-H. Lam, and F. C.-C. Ling, "Room temperature ferromagnetism in Sb doped ZnO," *J. Magn. Magn. Mater.*, 529, 167908, 2021.
- [15] H. Zhang, X. Y. Ma, Y. J. Ji, J. Xu, and D. R. Yang, "Single crystalline US nanorods fabricated by a novel hydrothermal method," *Chem. Phys. Lett.*, 377, 654-657, 2003.
- [16] H. Zhang, Y. J. Ji, X. Y. Ma, J. Xu, and D. R. Yang, "Long Bi<sub>2</sub>S<sub>3</sub> nanowires prepared by a simple hydrothermal method," *Nanotechnology*, 14, 974-977, 2003.

- [17] Y. Jiang, Y. Wu, S. Y. Zhang, C. Y. Xu, W. C. Yu, Y. Xie, *et al.*, "A catalytic-assembly solvothermal route to multiwall carbon nanotubes at a moderate temperature," *J. Am. Chem.*, 122, 12383-12384, 2000.
- [18] J. H. Zhan, X. G. Yang, D. W. Wang, S. D. Li, Y. Xie, Y. N. Xia, *et al.*, "Polymer-controlled growth of CdS nanowires," *Adv. Mater.*, 12 (8), 1348-1351, 2000.
- [19] F. Chouikh, Y. Beggah, and M. S. Aida, "Optical and electrical properties of Bi doped ZnO thin films deposited by ultrasonic spray pyrolysis," *J. Mater. Sci.: Mater. Electron*, 22, 499-505, 2011.
- [20] N. S. Kumar, K. V. Bangera, C. Anandan, and G. K. Shivakumar, "Properties of ZnO:Bi thin films prepared by spray pyrolysis technique," *J. Alloy. Compd.*, 578, 613-619, 2013.
- [21] C. H. Lee, K. S. Lim, and J. S. Song, "Highly textured ZnO thin films doped with indium prepared by the pyrosol method," *Sol. Energy Mater. Sol. Cells*, 43, 37-45, 1996.
- [22] M. Jiang, X. Liu, and H. Wang, "Conductive and transparent Bi-doped ZnO thin films prepared by rf magnetron sputtering," *Surf. Coat. Technol.*, 203, 3750-3753, 2009.
- [23] T. Ait Ahcene, C. Monty, J. Kouam, A. Thorel, G. Petot-Ervas, and A. Djemel, "Preparation by solar physical vapor deposition (SPVD) and nanostructural study of pure and Bi doped ZnO nanopowders," *J. Eur. Ceram. Soc.*, 27, 3413-3424, 2007.
- [24] E. F. Keskenler, S. Aydin, G. Turgut, and S. Dogan, "Optical and structural properties of bismuth doped ZnO thin films by sol-gel method: Urbach rule as a function of crystal defects," *Acta Phys. Polon. A*, 126, 782-786, 2014.
- [25] A. L. Patterson, "The Scherrer Formula for X-Ray Particle Size Determination," *Phys Rev.*, 56, 978-982, 1939.
- [26] K. Wu, Z. Jia, L. Zhou, S. Yuan, and J. Cui, "Study on the effect of methanol on the morphology and optical properties of ZnO," *Optik*, 205, 164250, 2020.
- [27] X. Xu, Y. Shen, N. Xu, W. Hu, J. Lai, Z. Ying, *et al.*, "Large-sized-mismatched group-V element doped ZnO films fabricated on silicon substrates by pulsed laser deposition," *Vacuum*, 84, 1306-1309, 2010.
- [28] V. S. Dharmadhikari, S. R. Sainkar, S. Badrinarayan, and A. Goswami, "Characterisation of thin films of bismuth oxide by X-ray photoelectron spectroscopy," *J. Electron. Spectrosc.*, 25, 181-189, 1982.
- [29] J. B. Zhong, J. Z. Li, Y. Lu, X. Y. He, J. Zeng, W. Hu, *et al.*, "Fabrication of Bi 3+-doped ZnO with enhanced photocatalytic performance," *Appl. Surf. Sci.*, 258, 4929-4933, 2012.